JOURNAL OF MATERIALS SCIENCE 30 (1995) 800–808

Characterization of vapour plume species and deposition residues resulting from pulsed laser ablation of a graphite/epoxy composite

R. E. ROYBAL, C. J. MIGLIONICO, C. STEIN
Space Environmental Interaction Branch, Phillips Laboratory, PL/VTSI, Kirtland Air Force Base, Albuquerque, NM 87117, USA

L. E. MURR
Department of Metallurgical and Materials Engineering, The University of Texas at El Paso, El Paso, TX 79968, USA

K. A. LINCOLN
Eloret Institute, NASA Ames Research Center, Moffett Field, CA 94035, USA

A modified time-of-flight mass spectrometer fitted with a special collection stage for carbon-coated transmission electron microscope specimen grids is used to monitor laser-pulse ablation products from graphite/epoxy composite targets. Scanning electron microscopy observations show ablation damage to consist of matrix pyrolysis, fibre fracture and spallation of fragments which include elemental hydrogen, carbon epoxide and acetylene groups. Transmission electron microscope examination of specimen grids showed a variety of crystals and polycrystalline hexagonal graphites having a wide range of shapes including spheres and faceted polyhedra and platelets, textured flake structures, and microrosettes. These observations lend some credibility to a model for laser-shock and pyrolysis effects which create molecular plume fragments and deposition fragments of hexagonal graphite.

1. Introduction

There has been considerable interest over the past several decades in the interactions of laser beams with a variety of materials, especially those involved in aerospace applications [1, 2]. More recently these interactions have been of particular interest in the context of space defence systems such as the US Strategic Defense Initiative (Starwars) and laser blow-off of spacecraft materials [3], especially laser–composite interactions. These interactions can involve a variety of energy deposition phenomena which include laser shock effects (including shock pressure effects, spallation, and shock heating) [4], and constrained plasma (pyrolysis) effects [5] which can lead to a host of chemical effects, blow-off of discrete matter, and deposition of recombined components (including molecular fragments) as well as direct or redeposition of molecular fragments [6]. Earlier efforts to investigate some of the phenomena involving laser blow-off of spacecraft materials attempted to develop analytical methodologies to predict target materials response to repetitive (pulsed) laser irradiation. These methodologies included the vapour plume characterization: velocity, expansion angle and mass fraction. These more recent investigations, unlike those originally conceived simply to explore degradation of target materials in laser impact situations [1, 2], have been more concerned with the contamination of neighbouring surfaces by deposition of interaction and reaction products. The specific concerns in these processes include the contamination or alteration of sensor, optical, or other protective surfaces by blow-off or plume debris.

In the research reported here, a time-of-flight mass spectrometer (TOFMS) analytical technique developed at NASA Ames Research Center dynamically to sample vapour plumes was modified to collect deposition fractions (or fragments) of plumes from a pulsed-laser-irradiated graphite-epoxy (G/E) composite. This technique included a TOFMS equipped with a special collection system employing carbon support grids which would collect deposited plume material that could be examined in a transmission electron microscope. In this way we hoped to examine the ablation site, plume composition, and any residual deposition fragments.

2. Experimental procedure

In this investigation a TOFMS capable of producing time-resolved spectra along the duration of a vapour plume was incorporated into a pulsed-laser/materials interaction chamber as shown in Fig. 1. The laser wavelength was 1.06 μm with a pulse duration of 800 μs. The beam was directed into the chamber with

0022–2461

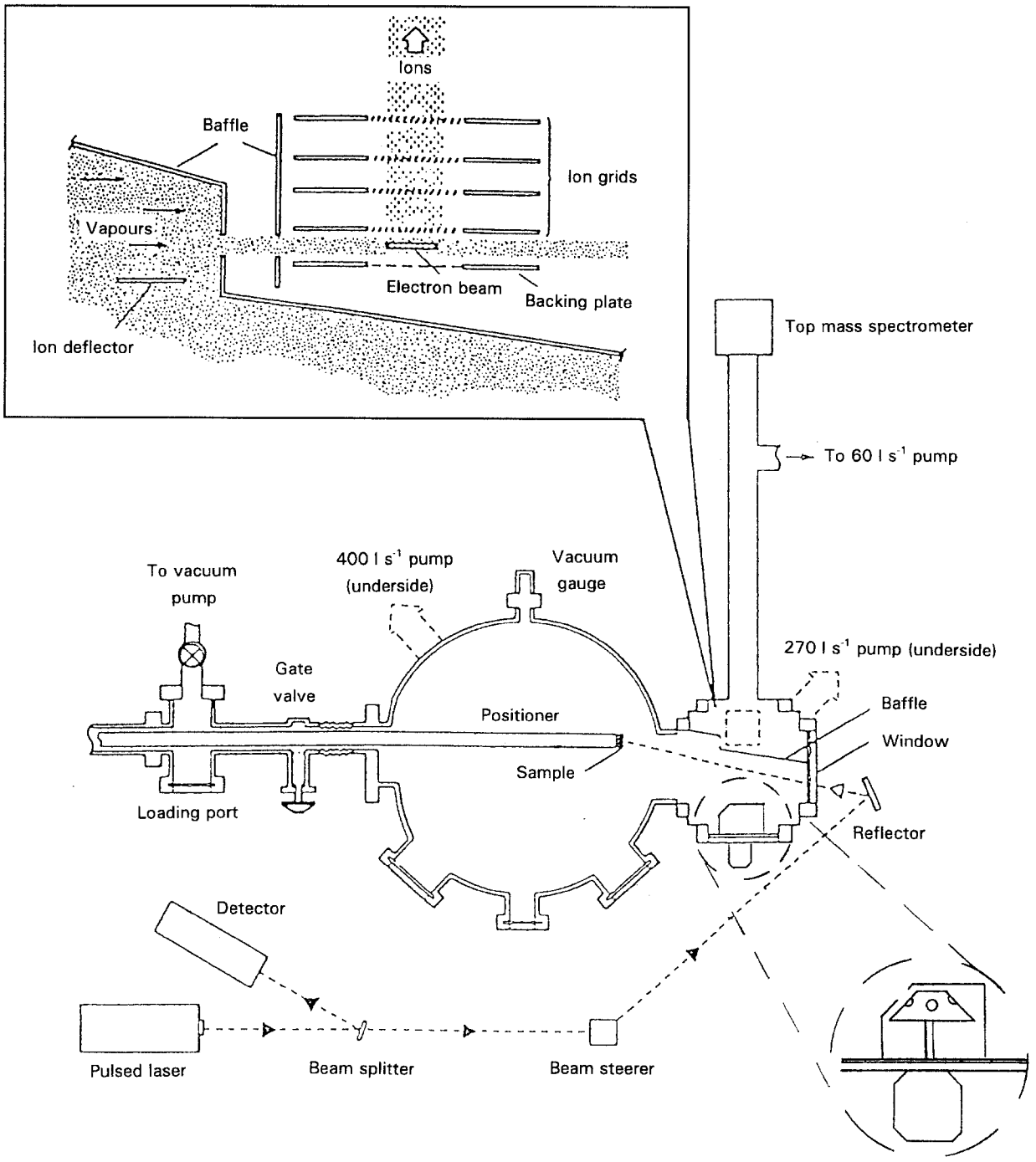

Figure 1 Schematic diagram of the advanced laser/time-of-flight mass spectrometer system with TEM grid specimen collection stage.

a series of lens to maintain a spot size of 6 mm^2. Samples were irradiated with single pulses and their "vapour pulse" spectra examined in the TOFMS.

The collection grids for transmission electron microscopy (TEM) were examined following single and multiple-pulse experiments. These examinations involved both conventional and scanning transmission electron microscopy (CTEM and STEM) which included energy-dispersive X-ray spectrometry, selected-area electron diffraction and microdiffraction analysis, and lattice imaging of deposited, electron transparent fragments.

3. Results and discussion

Fig. 2 presents a rather practical (and macroscopic) overview of the laser-graphite/epoxy (G/E) target materials interaction involving localized damage to the irradiated focal area on the specimen surface. These residual damage microstructures show graphite fibre fracture and matrix ablation. Evidence of local melt or vapour redeposition is also illustrated.

Fig. 3 is a typical, multi-shot mass spectrum averaged from 15 time-resolved spectra resulting from a single laser shot on a target such as those illustrated in Fig. 2. There are several notable features (pyrolysis products) of this spectrum: free hydrogen, free carbon, epoxide fragments (free radicals), acetylenes (fixed gases) and impurities. Other notable fragments include CH, CH_2 and CH_3 groups. These constituents can be visualized with the aid of some generalized chemical structures for epoxy resins illustrated in Fig. 4. The epoxide group (C_2H_3O) shown contains a covalent half-bond available for bonding. For solid

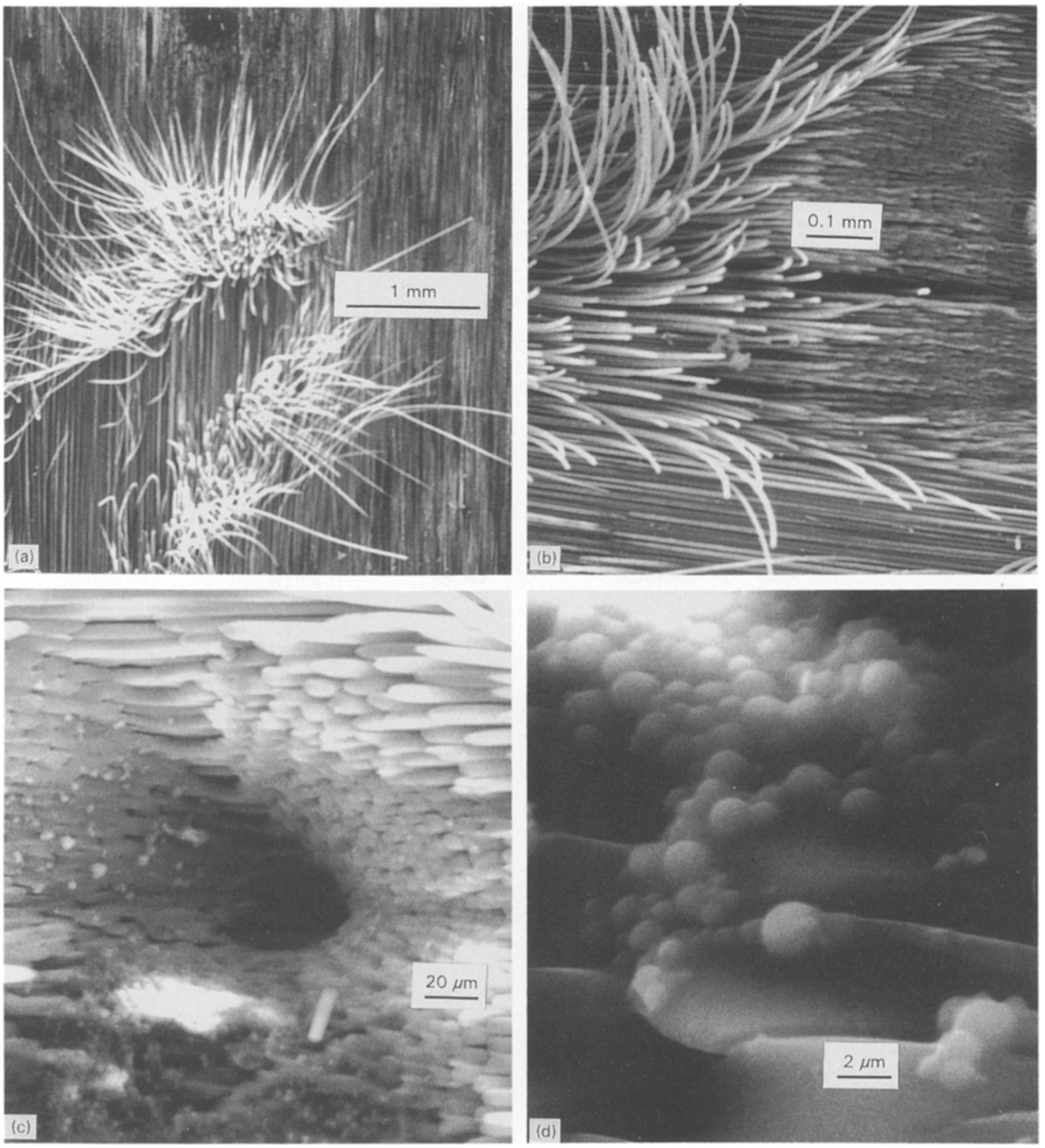

Figure 2 SEM views of laser-ablated graphite/epoxy specimen areas. (a, b) Broken, exposed graphite fibres in ablation zone; (c) ablation tunnel showing fibre damage detail, (d) melt/deposition hemisphere growth in ablation zone.

resins, n in Fig. 4 is 2 or greater. The epoxy and hydroxyl groups (–OH) are the reaction sites for cross-linking.

The presence of contaminants such as sodium, potassium, iron, calcium, chlorine, aluminium and water vapour (H_2O) occur primarily on or very near the specimen surface, and this is illustrated to some extent by comparing the time-resolved spectral arrays from the first laser shot (Fig. 5a) to that of the fourth laser shot (Fig. 5b) on the same area. These show a reduction in water vapour and removal of surface contaminants as a result of the multiple shots. Fig. 5 also shows a marked reduction in the epoxide component with repeated laser pulsing and an increase in C_n and the acetylene family fragments. The resulting ablation sequence after larger numbers of pulses generally showed spectra typical for graphitic materials [8].

When looking at the vapour plume in a time-resolved fashion as in Fig. 5, it was found that the species possessed different generation times and lifespans. The expected order of species generation was epoxides, acetylene, and finally carbons. This was based on the corresponding heats of formation of the different species ($HCH_3 = 30$ kcal mol^{-1}: $H_{acetylene} = 52$ kcal mol^{-1}; $H_{C_3} = 178$ kcal mol^{-1}). In fact the carbons were generated before the acetylenes. C_3 was assumed to be a product of laser decomposition

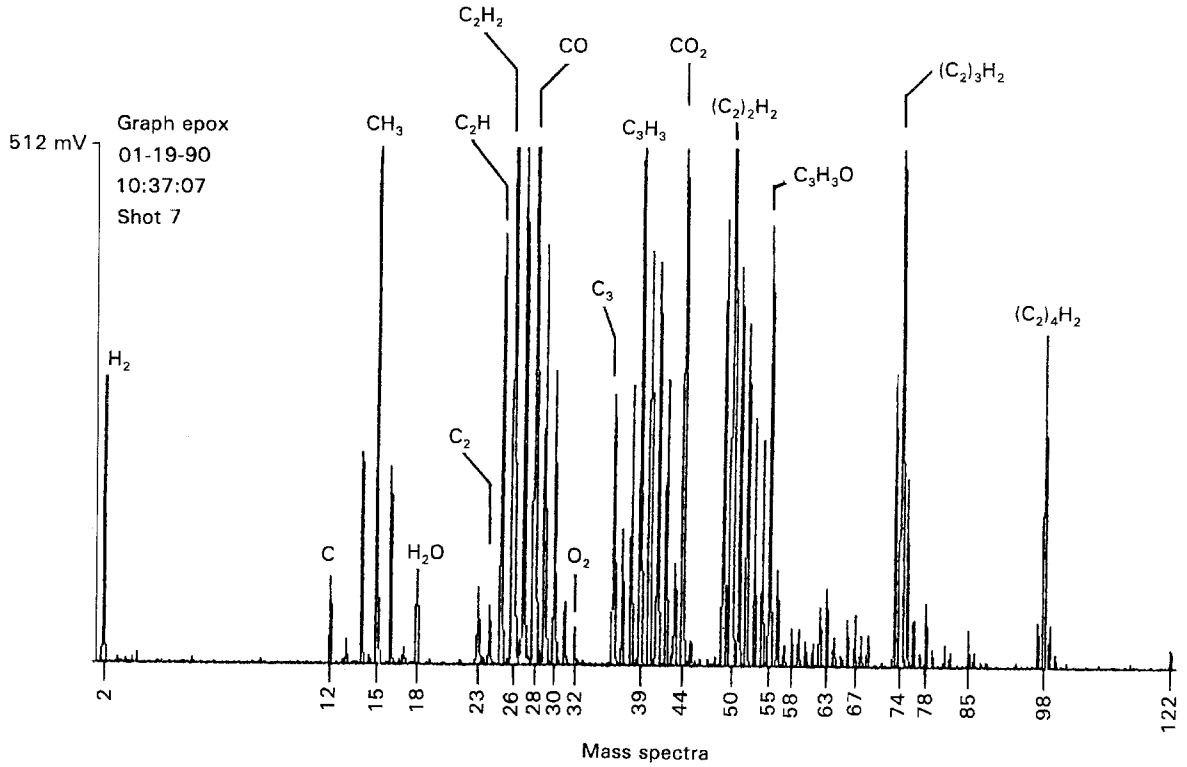

Figure 3 TOFMS spectrum for ablation plume characterization showing typical mass spectrum (mass-to-charge ratio)/fragment analysis after seven pulses.

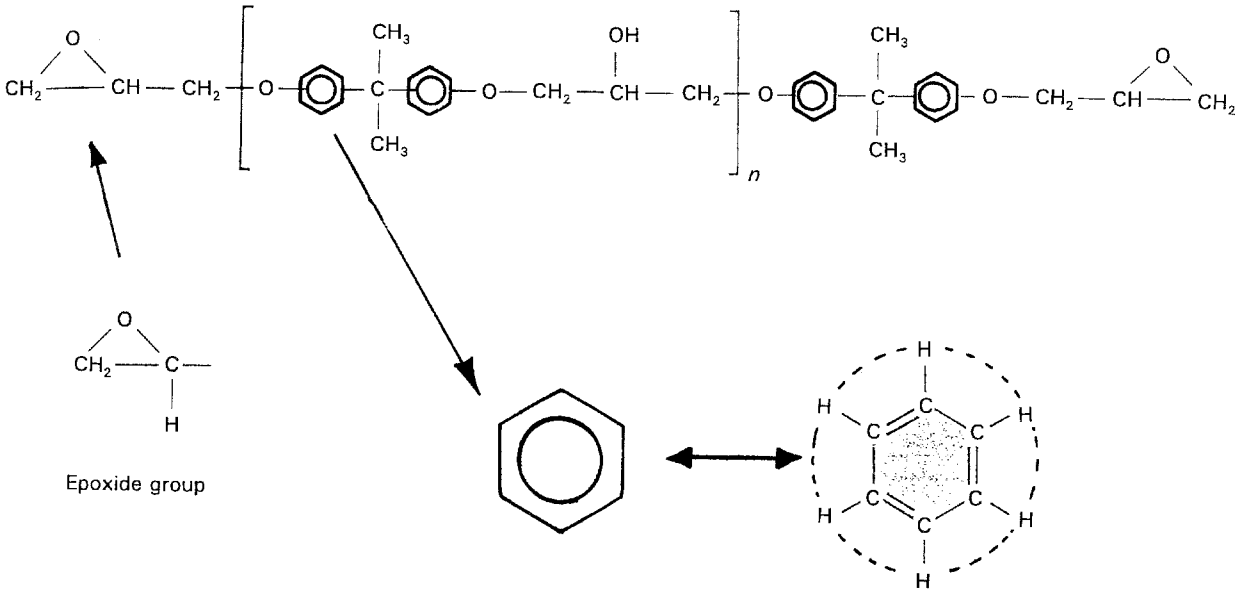

Figure 4 Simple epoxy chemical structure showing epoxide group and benzene-ring-containing polymer structure groups. Circles and dotted circles represent hydrogen groupings or delocalized electron bonding within the benzene ring.

of the epoxide component deposited on the sample surface.

The surface vaporization temperature of the C_3 component, for example, can be calculated from a simple gas dynamic model for a hypersonic free jet expanding adiabatically, as illustrated previously by Lincoln and Covington [9] to be about 4000 K. The C_3 also apparently emanates as free radicals but with less affinity than the epoxides. The moderate lifespans of carbon seen in the TOFMS spectra may be attributed to the fact that C_3 is a condensable. This is represented by the shorter of the C_3 spectrum in the time versus intensity data illustrated in Fig. 5. On examining the carbon grid surfaces by TEM, a variety and distribution of deposited "particles" were observed. These particulates assumed a variety of morphologies ranging from apparent "spheres" to faceted polyhedra, and plate-like morphologies to sheet-like fragments. Some individual particles aggregated, and some of these aggregates contained contaminating particulates. Many aggregates contained growth features such as rosettes and spiral structures typical of high-quality (pure) graphites [10]. These morphological features are illustrated in the examples reproduced in Figs 6–8.

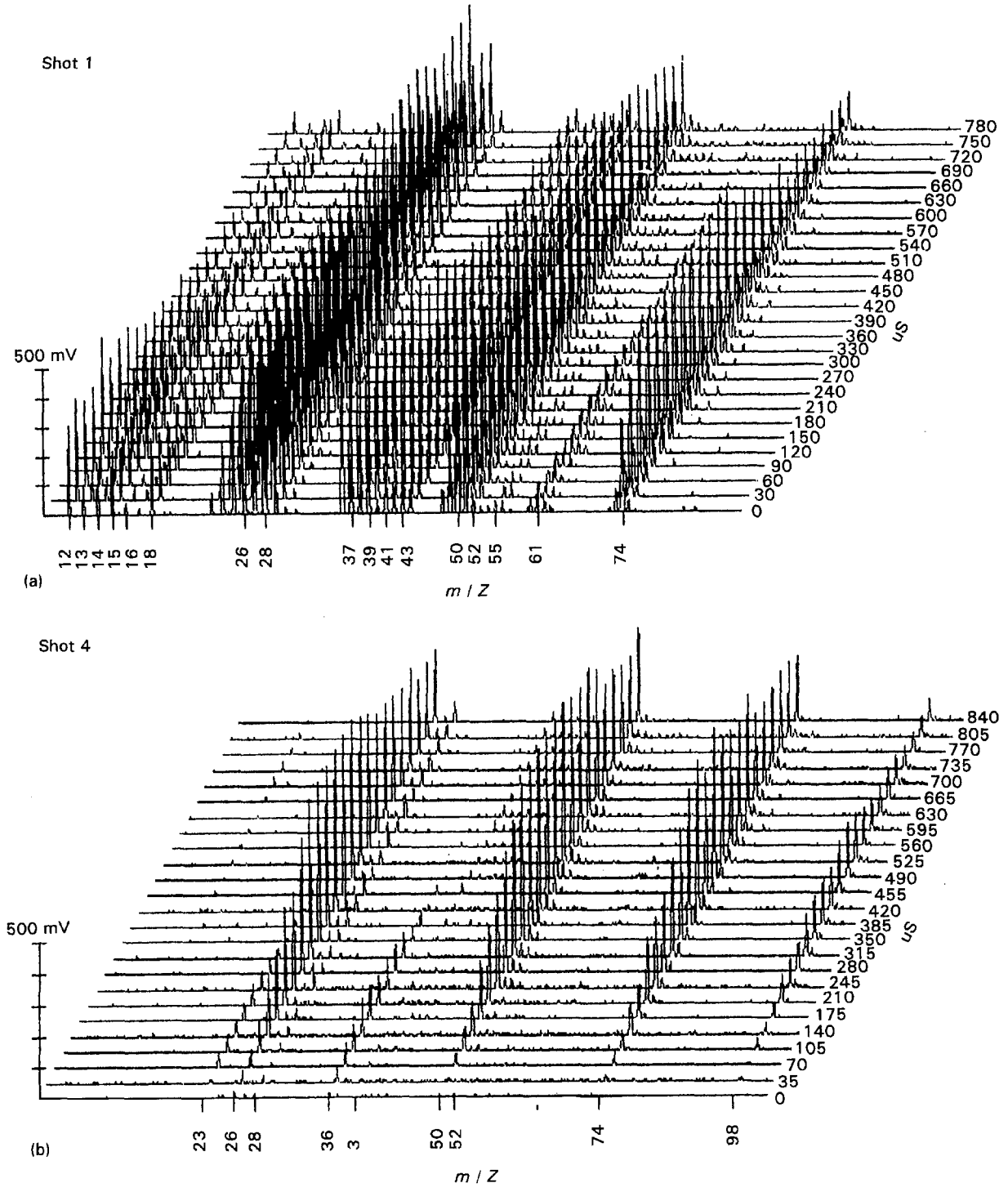

Figure 5 Time-resolved TOFMS spectra comparing (a) spectra generated by a single pulse, and (b) spectra generated after four pulses.

The crystallographic features of graphite unique and implicit to some extent in Figs 6–8 are illustrated in more detail in the examples shown in Figs 9 and 10. These examples, together with those shown in Figs 6–8, suggest a wide range of graphite ablation fragments either as a direct consequence of graphite fibre damage or "condensation" of carbon fragments in the plume composition from the epoxy matrix. The TEM observations in Figs 6–10, taken together with the plume spectra shown in Figs 3 and 5, suggest a complex set of ablation-related phenomena which include both the graphite fibres and the deposition of graphite blow-off fragments which result by laser-induced decomposition (pyrolysis) of the epoxy matrix. Indeed, it is well known that destructive shockwave reactions/interactions can break molecular bonds leading to either isomerization or polymerization [11, 12]. In the crystallization of low molecular weight fractions from the melt at high temperatures it is possible to obtain extended chain crystals in which the distribution of crystal thickness approximates the distribution of chain lengths [13]. A polymer molecule in the vicinity of a surface has its entropy decreased and its free energy increased in comparison to a molecule not so impeded [14]. Consequently, the combination of localized high temperature, shock spallation and shock heating as well as shock energy localization can cause

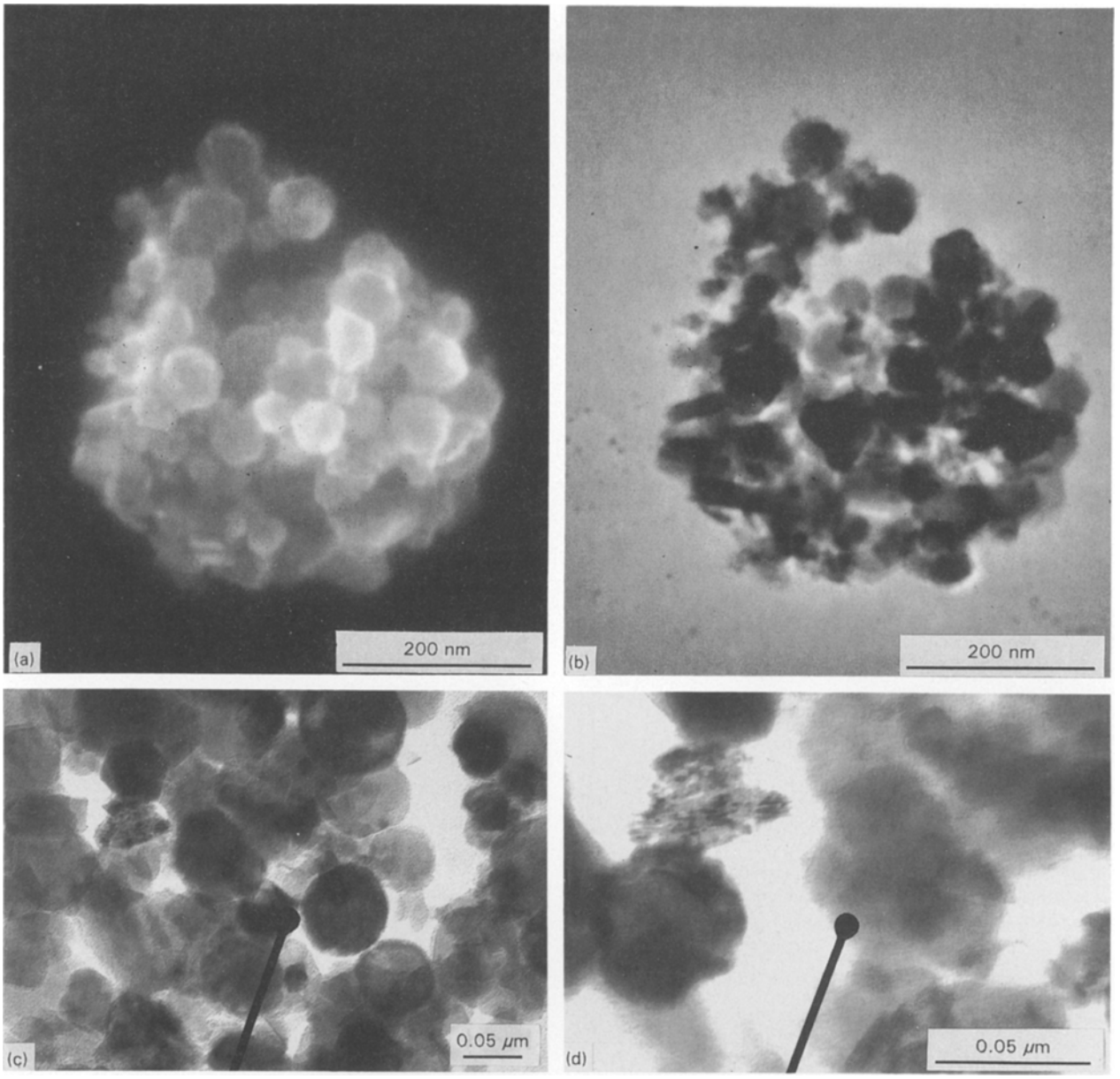

Figure 6 Examples of graphite deposition residue (particulates) collected on TEM carbon-coated grids. (a) Secondary electron (SEM-mode) image, and (b) STEM-mode image of particle cluster. (c) Hexagonally faceted graphite particles observed in CTEM mode. (d) Variations of CTEM particle images.

fragmentation and recombination (condensation) as illustrated in Fig. 11. This process produces a wide range of crystalline and polycrystalline (hexagonal) graphite particulates and aggregates as illustrated in Figs 6–10, and consistent with the spectra shown typically in Fig. 3. While other carbon variants were investigated (such as the higher forms of C_n: C_{40}, C_{60}, C_{70}, etc.) the analyses only identified various forms (crystallinity and polycrystallinity in a variety of morphologies ranging from spheroids to platelets) of hexagonal graphite.

4. Conclusion

SEM was used to examine the macroscopic features of laser ablation damage to a graphite/epoxy composite along with time-of-flight mass spectrometry to examine the pulsed plume emission during ablation, and TEM to observe debris and deposition fragments resulting from the ablation process. The total picture which emerges from these observations involves laser shock damage fragments along with pyrolysis components, all of which are finally deposited some distance ($\sim$ 13 cm) from the ablation zone. These deposited particulates include a wide range of hexagonal graphite morphologies and crystal structures which include direct fragmentation (or spallation) from the graphite fibres in the composite along with shock and pyrolysis-induced graphites which originate from the molecular fragmentation and carbon condensation from the epoxy matrix.

While it is impossible to separate explicitly the shock-induced and pyrolysis-induced deposition of graphite particulates on surfaces away from the ablation zone, it might be assumed that similar phenomena would occur in hypervelocity particle impacts with graphite/epoxy composite materials in space. The important aspects of these ablation and hypervelocity

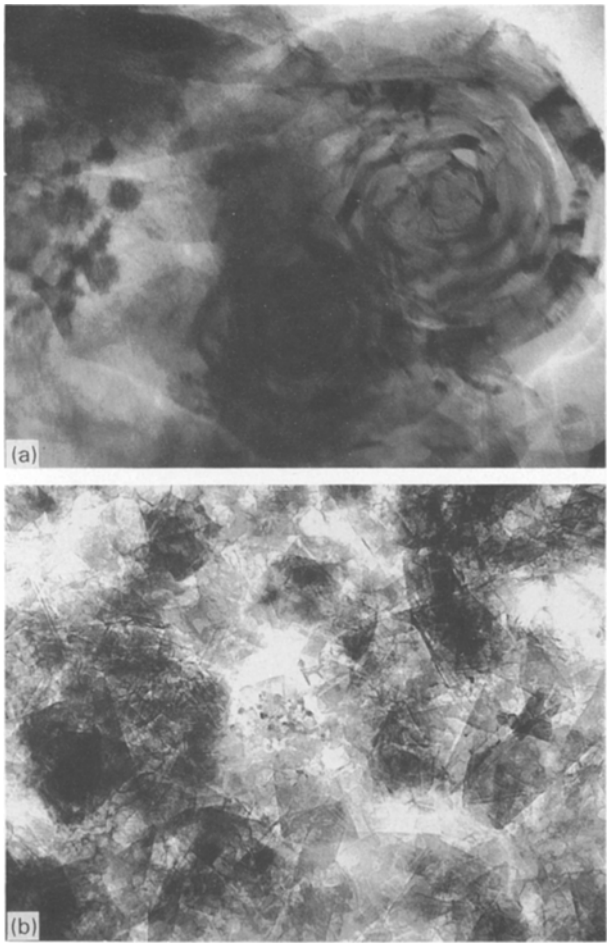

Figure 7 (a) Rosette and (b) thin flake (plate-like) graphite particles deposited on carbon-coated grids in ablation blow-off plume as observed by TEM (bright-field images).

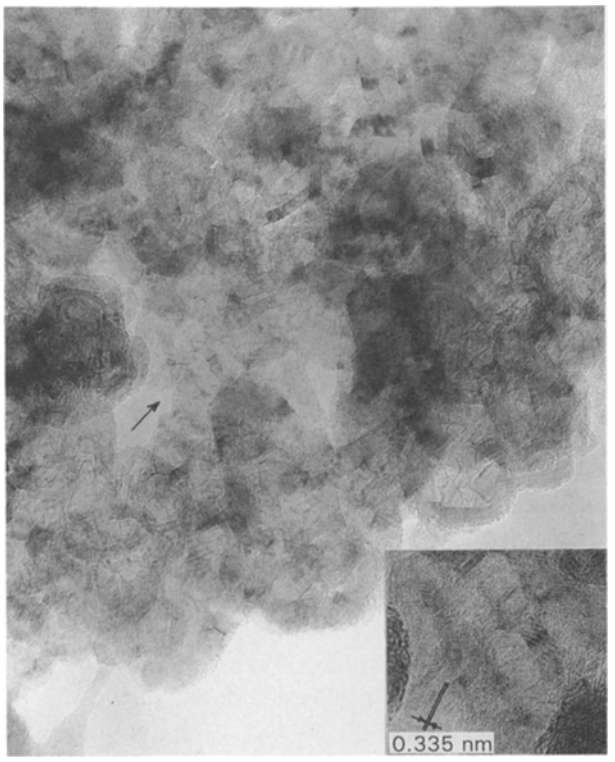

Figure 8 Standard, high-purity graphite lattice-image standard showing growth features and polycrystalline structures. Inset shows lattice image details for micro-rosette growth.

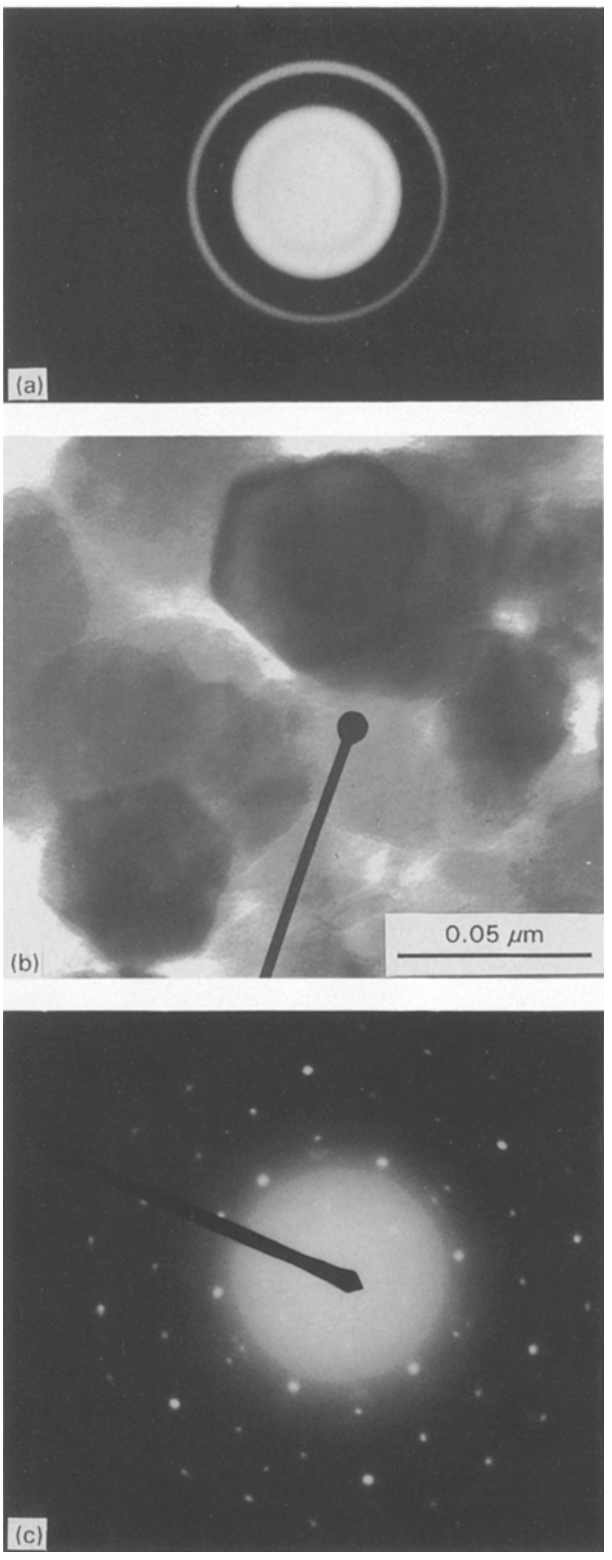

Figure 9 Crystallinity and crystal morphology in deposited (hexagonal) graphite. (a) "Amorphous" reference diffraction pattern for the carbon support film composing the TEM grid collector. (b) TEM (bright-field) image showing facets characteristic of hexagonal graphite crystals oriented parallel to basal (0 0 0 1) plane confirmed by the selected-area electron diffraction spot pattern in (c).

impact phenomena are concerned with the potential for alteration, compromising or degradation of sensor, optical or control surfaces as a consequence of graphite deposition from a vapour plume. This scenario may be especially important in altering the electrical conductivity of a neighbouring component as a

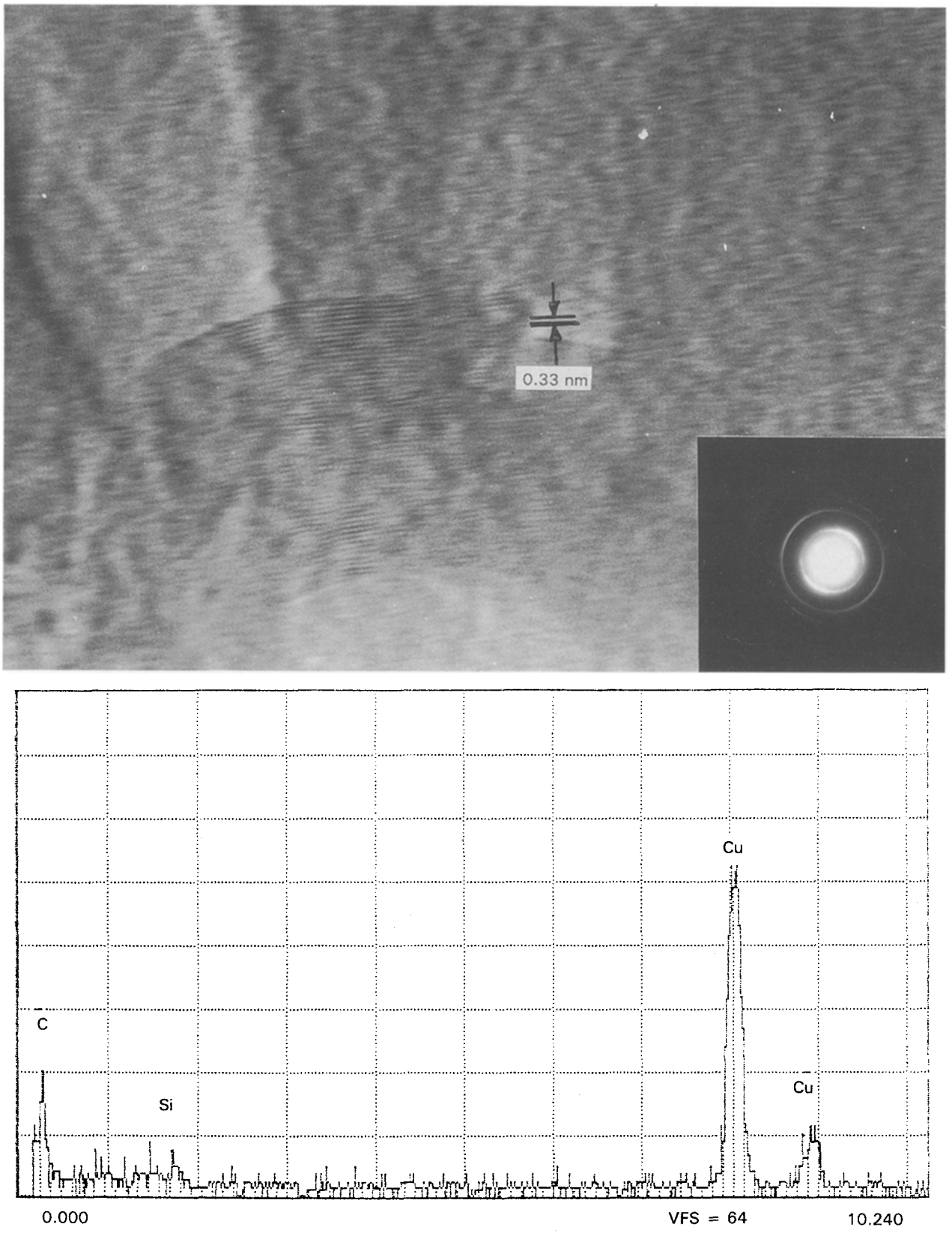

Figure 10 Polycrystalline and textured (oriented) graphite platelets showing lattice fringes for (0 0 0 2) basal plane spacing. The selected-area electron diffraction pattern inset shows the polycrystalline, fine crystal texture implicit in the TEM image while the energy-dispersive X-ray spectrum shows the elemental carbon peak characteristic of the graphite structure. The copper peaks represent the copper support grid and serve as a calibration standard.

consequence of graphite deposition from impacted polymeric materials in general if elemental carbon is redeposited as graphite. In this regard, there was no evidence in this work for other, higher-carbon complexes (fullerenes) such as C_{40}, C_{60}, C_{70}, etc., or of crystalline diamond.

Acknowledgements

The authors are grateful to Drs A. H. Advani and C-S. Niou for their help with some of the TEM sample analyses. This work was supported in part by NASA-Johnson Space Center Grant NAG 9-481.

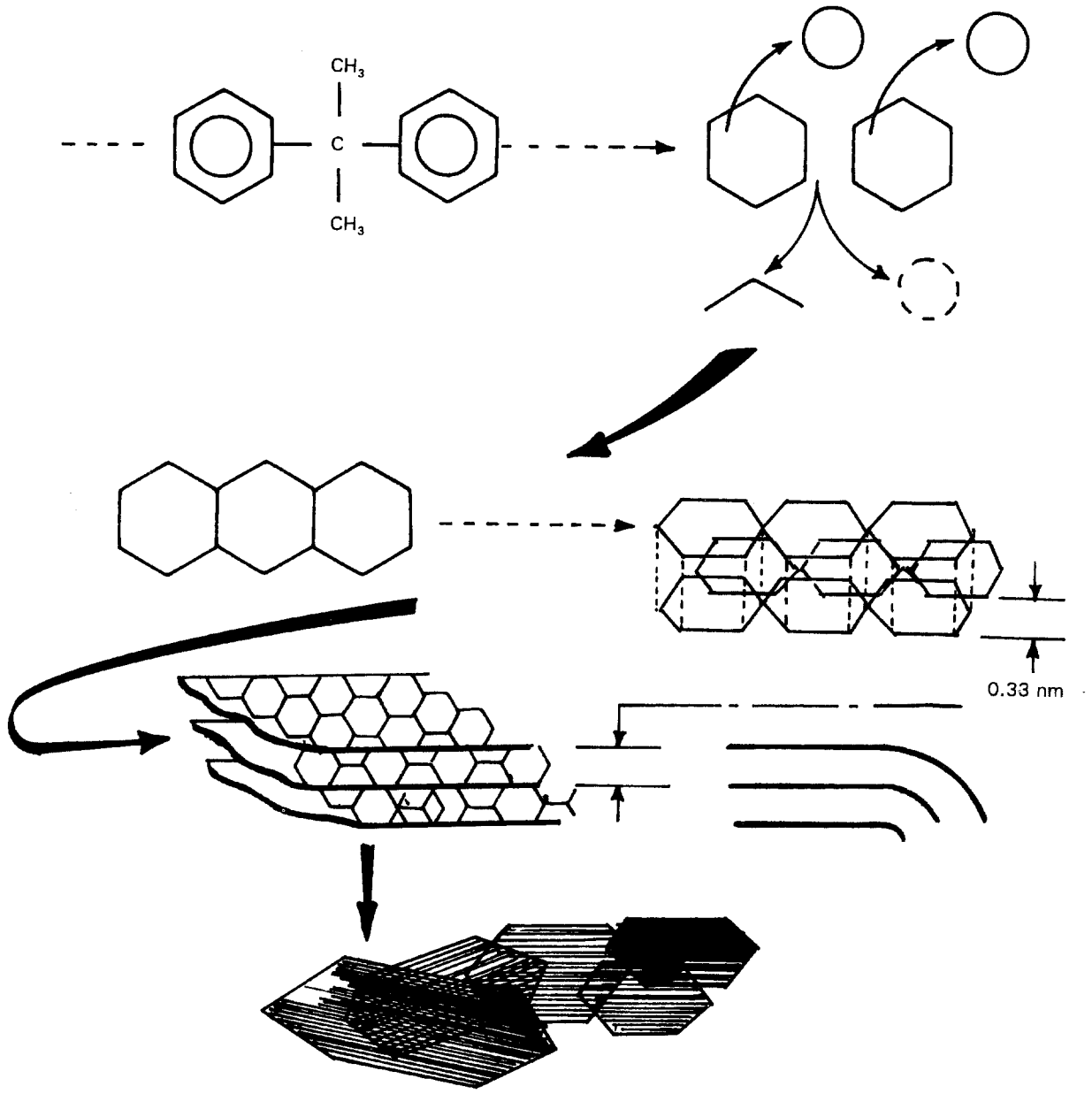

Figure 11 Schematic representation of a simple molecular fragmentation model to produce graphite particulates in the ablation blow-off plume for laser-irradiated graphite/epoxy composite. In this simple model, laser-shock-induced hydrogen fragmentation (rings) leaves C_3 and C_6 (benzene) groups which recombine to form various shapes and periods of crystalline and polycrystalline hexagonal graphites.

References

1. A. J. GLASS and A. H. GUENTHER (eds), "Damage in Laser Glass", ASTM Special Technical Publication 469 (ASTM, Philadelphia, PA, 1969).
2. *Idem*, "Laser Induced Damage in Optical Materials", NBS Special Publication 462 (ASTM Special Technical Publication 622) (US Government Printing Office, Washington DC., 1976).
3. I. RUBIN and M. S. CHOU, "Repetitively Pulsed Laser Effects Phenomenology Program", AFWL-TR-88-112 (Kirtland AFB NH, 1987).
4. A. H. CLAUER, J. H. HOLBROOK and B. P. FAIRAND, in "Shock Waves and High-Strain-Rate Phenomena in Metals", edited by M. A. Meyers and L. E. Murr (Plenum Press, New York, 1981) p. 675.
5. S. S. BATSANOV, "Physical Chemistry of Shock-Induced Compression: A New Scientific Trend Comes into Being" (Izvestia, Siberian Academy of Sciences Chemical Series, 1967) p. 676.
6. S. S. BATSANOV, *Russ. Chem. Rev.* **55**(4) (1986) 297.
7. K. A. LINCOLN and R. D. BECHTEL, "A Fast Data Acquisition System for the Study of Transient Events by High Repetition Rate Time-of-Flight Mass Spectrometer", NASA Technical Memorandum 88374 (1986).
8. K. A. LINCOLN, *AIAA J.*, **21**(8) (1983) 1204.
9. K. A. LINCOLN and A. M. COVINGTON, *Int. J. Mass Spectr. Ion. Proc.* **16** (1975) 191.
10. S. IIJIMA, *J. Phys. Chem.* **91** (1987) 3466.
11. W. HERMANN, *J. Appl. Phys.* **40** (1969) 2490.
12. T. SEKINE, in "Shock-Wave and High-Strain Rate Phenomena in Materials", edited by M. A. Meyers, L. E. Murr and K. P. Staudhammer (Marcel Dekker, New York, 1992) p. 311.
13. F. C. ANDERSON, *J. Appl. Phys.* **35** (1964) 64.
14. P. H. LINDENMEYER, in "Frontiers in Materials Science", edited by L. E. Murr and C. Stein (Marcel Dekker, New York, 1976) p. 219.

Received 6 April 1993
and accepted 26 April 1994